Synaptotagmin-7 is a key factor for bipolar-like behavioral abnormalities in mice

Wei Shen[a,1], Qiu-Wen Wang[a,1], Yao-Nan Liu[a,1], Maria C. Marchetto[b], Sara Linker[b], Si-Yao Lu[a], Yun Chen[a], Chuihong Liu[c], Chongye Guo[d,e], Zhikai Xing[d,e], Wei Shi[f], John R. Kelsoe[g], Martin Alda[h], Hongwei Wang[i], Yi Zhong[j], Sen-Fang Sui[k], Mei Zhao[l,m], Yiming Yang[n], Shuangli Mi[d,e], Liping Cao[c], Fred H. Gage[b,2], and Jun Yao[a,2]

[a]State Key Laboratory of Membrane Biology, Tsinghua-Peking Center for Life Sciences, IDG/McGovern Institute for Brain Research, School of Life Sciences, Tsinghua University, 100084 Beijing, China; [b]Laboratory of Genetics, The Salk Institute for Biological Studies, La Jolla, CA 92037; [c]Guangzhou Huiai Hospital, Affiliated Brain Hospital of Guangzhou Medical University, 510370 Guangzhou, Guangdong, China; [d]Key Laboratory of Genomic and Precision Medicine, Beijing Institute of Genomics, Chinese Academy of Sciences, 100101 Beijing, China; [e]University of Chinese Academy of Sciences, 100049 Beijing, China; [f]Beijing Advanced Innovation Center for Big Data-based Precision Medicine, Beihang University, 100191 Beijing, China; [g]Institute for Genomic Medicine, University of California San Diego, La Jolla, CA 92093; [h]Department of Psychiatry, Dalhousie University, Halifax, NS B3H 2E2, Canada; [i]Tsinghua-Peking Center for Life Sciences, School of Life Sciences, Tsinghua University, 100084 Beijing, China; [j]Tsinghua-Peking Center for Life Sciences, IDG/McGovern Institute for Brain Research, School of Life Sciences, Tsinghua University, 100084, Beijing, China; [k]State Key Laboratory of Membrane Biology, Beijing Advanced Innovation Center for Structural Biology, School of Life Sciences, Tsinghua University, 100084 Beijing, China; [l]Key Lab of Mental Health, Institute of Psychology, Chinese Academy of Sciences, 100101 Beijing, China; [m]University of Chinese Academy of Sciences, 101408 Beijing, China; and [n]School of Linguistic Sciences and Arts, Collaborative Innovation Center for Language Ability, Jiangsu Normal University, 221009 Xuzhou, Jiangsu, China

Contributed by Fred H. Gage, January 12, 2020 (sent for review October 17, 2019; reviewed by Ronald S. Duman and Eric J. Nestler)

The pathogenesis of bipolar disorder (BD) has remained enigmatic, largely because genetic animal models based on identified susceptible genes have often failed to show core symptoms of spontaneous mood cycling. However, pedigree and induced pluripotent stem cell (iPSC)-based analyses have implicated that dysfunction in some key signaling cascades might be crucial for the disease pathogenesis in a subpopulation of BD patients. We hypothesized that the behavioral abnormalities of patients and the comorbid metabolic abnormalities might share some identical molecular mechanism. Hence, we investigated the expression of insulin/synapse dually functioning genes in neurons derived from the iPSCs of BD patients and the behavioral phenotype of mice with these genes silenced in the hippocampus. By these means, we identified synaptotagmin-7 (Syt7) as a candidate risk factor for behavioral abnormalities. We then investigated Syt7 knockout (KO) mice and observed nocturnal manic-like and diurnal depressive-like behavioral fluctuations in a majority of these animals, analogous to the mood cycling symptoms of BD. We treated the Syt7 KO mice with clinical BD drugs including olanzapine and lithium, and found that the drug treatments could efficiently regulate the behavioral abnormalities of the Syt7 KO mice. To further verify whether Syt7 deficits existed in BD patients, we investigated the plasma samples of 20 BD patients and found that the Syt7 mRNA level was significantly attenuated in the patient plasma compared to the healthy controls. We therefore concluded that Syt7 is likely a key factor for the bipolar-like behavioral abnormalities.

synaptotagmin-7 | induced pluripotent stem cell | mental disorder | bipolar disorder

Clinical research has identified a number of susceptible genes that might be involved in the inheritance and pathogenesis of bipolar disorder (BD) (1). For instance, mice expressing a mutant form CLOCK gene, which was identified in a subpopulation of BD patients, showed behavioral abnormalities that are similar to human mania (2). However, these genes account for only a very small proportion of clinical cases, and genetic animal models based on them have not been able to show spontaneous cycling of manic and depressive moods, which is the core symptom of BD (3, 4). These reports support the hypothesis that BD requires accumulative consequences of deficits in multiple genes that may be distributed diversely across the genome (5, 6). Interestingly, pedigree analyses have suggested a strong heritability of BD, indicating that the molecular and cellular deficits key for the mood abnormalities within the family can be stably inherited. In addition to bidirectional mood abnormalities, another important feature of BD is that ∼40% of BD patients suffer from insulin/glucose metabolic comorbidities (7–9). Although a hypothesis of insulin deficits has been proposed to explain the occurrence of depressive disorder in diabetes patients (10), the exact mechanisms linking the neural and metabolic deficits in BD patients have remained poorly understood. However, given the generally homologous behavioral and metabolic symptoms shown by BD patients, it is possible that a subpopulation of patients might share the pathogenic molecular and cellular deficits, despite their diverse genetic deficiencies.

In recent years, accumulating evidence has suggested that synaptic proteins are involved in mental disorders including BD, as revealed through genetic variants, gene expression changes, or target therapy efficacy (11–14). For instance, ketamine, an NMDAR antagonist that has been clinically approved for the treatment of depressive disorders, has been suggested to have antidepressant effects probably through the shutdown of the GluN2B subunit (15–18). Synaptotagmin-7 (Syt7) appears to play important roles in both the synaptic transmission in the brain and

Significance

The key molecular mechanisms underlying the etiology of bipolar disorder (BD) have remained enigmatic. As BD patients often show comorbidity with insulin/glucose metabolic syndrome, we hypothesized that the central and peripheral abnormalities might share some identical molecular mechanism. Through investigating the expression of insulin/synapse dual functioning genes in patient induced pluripotent stem cell-derived neurons and their effects on mouse behaviors, as well as testing the mRNA level in BD patient plasma samples, we demonstrated that Syt7 is likely a key factor involved in neuropsychiatric-like behaviors. Our work helps explain the molecular mechanism involved in the pathogenesis of BD.

Author contributions: J.Y. designed research; W. Shen, Q.-W.W., Y.-N.L., M.C.M., S.L., S.-Y.L., Y.C., C.L., C.G., Z.X., W. Shi, J.R.K., M.A., H.W., Y.Z., S.-F.S., M.Z., Y.Y., S.M., and L.C. performed research; W. Shen, Q.-W.W., Y.-N.L., and J.Y. analyzed data; and F.H.G. and J.Y. wrote the paper.

Reviewers: R.S.D., Yale University School of Medicine and US Department of Veterans Affairs; and E.J.N., Icahn School of Medicine at Mount Sinai.

The authors declare no competing interest.

[1]W. Shen, Q.-W.W., and Y.-N.L. contributed equally to this work.

[2]To whom correspondence may be addressed. Email: gage@salk.edu or jyao@mail.tsinghua.edu.cn.

This article contains supporting information online at https://www.pnas.org/lookup/suppl/doi:10.1073/pnas.1918165117/-/DCSupplemental.

First published February 10, 2020.

insulin metabolism in the pancreas. Syt7 drives the exocytosis of secretory vesicles through its two tandem Ca^{2+}-binding domains interacting with Ca^{2+}, SNAREs and phospholipids. In the brain, Syt7 deficiency causes an attenuation of AP-triggered asynchronous synaptic vesicle (SV) release, SV endocytosis and replenishment, and synaptic facilitation in the presynaptic nerve terminals, as well as AMPAR trafficking in the postsynaptic density (19–24). In pancreatic β-cells, Syt7 plays an essential role in promoting insulin secretion (25), and the glucagon-like peptide-1 (GLP-1) pathway, one therapeutic target of T2D drugs, can up-regulate the phosphorylation of Syt7 to facilitate insulin secretion (26).

In the present study, we hypothesized that, in patients suffering a psychiatric disorder like BD, the neuropsychiatric abnormalities in the brain and the insulin metabolic defects in the periphery might be attributable to identical molecular mechanisms. By investigating the expression of genes that have been reported to be involved in both insulin metabolism and neurotransmission in the BD patient iPSC-derived dentate gyrus (DG)-like neurons and their effects on the psychiatric behaviors of mice, we identified Syt7 as a candidate risk factor for the linkage of central and peripheral abnormalities. We then systematically investigated the behavioral defects of the Syt7 KO mice and found that the Syt7 KO mice showed manic-like behavioral abnormalities in the dark phase and depressive-like behavioral abnormalities in the light phase. Furthermore, the behavioral abnormalities shown by the Syt7 KO mice could be efficiently treated by mood stabilizing drugs, namely olanzapine and lithium. Finally, to investigate whether the insufficient Syt7 expression detected in the iPSC-derived neurons existed in BD patients, we tested the plasma samples of 20 BD patients and found that the Syt7 mRNA level was attenuated in the patient plasma compared to the healthy controls. Therefore, our results indicated that Syt7 probably plays a key role in bipolar-like behavioral abnormalities.

Results

Identification of Syt7 as a Candidate Risk Factor for Neuropsychiatric-like Behaviors. To efficiently identify the molecules that contribute significantly to the mood abnormalities in BD patients, we chose to investigate the expression and function of those genes involved in the comorbidities of BD in the patient iPSC-derived neurons. Approximately 40% of BD patients suffer from insulin/glucose metabolic syndrome (7–9). We hypothesized that deficits in the key molecular pathway in the brain can induce behavioral symptoms, whereas they can generate insulin metabolic symptoms if they occur in the islets, which might be one reason why the two diseases can be comorbid (Fig. 1*A*). We thus searched the GeneCards database using the keywords insulin (or diabetes) and synapse and found 97 genes that might be involved in both insulin metabolism and synaptic function. Through verification with literature searching using the National Center for Biotechnology Information database (https://www.ncbi.nlm.nih.gov/pubmed/), we determined that 18 of the 97 genes were likely associated with dual functions. Previously, we had established the iPSC and hippocampal DG-like neuron models for six BD-I patients (27). In the neurons derived from the patient iPSCs, 11 of the 18 genes showed a ≥1.5-fold change in the mRNA expression, as evidenced by RNA-sequencing (seq) and qRT-PCR analyses (Fig. 1 *B* and *C*). We then knocked down the 11 genes in the DG of mice by introducing the small hairpin RNA (shRNA)-encoding lentivirus and analyzed the immobility time of the mice during a forced swim test (FST), which has been widely used to study the responses of animals to acute stress. The results indicated that, compared to the WT group, the Syt7 knockdown (KD) mice showed a significantly reduced immobility time, whereas the animals with other KD genes failed to show any obvious changes (Fig. 1*D*). We further carried out an open field test (OFT) to investigate the locomotor activity of the mice with candidate gene KD. We observed that among the 11 test groups, only

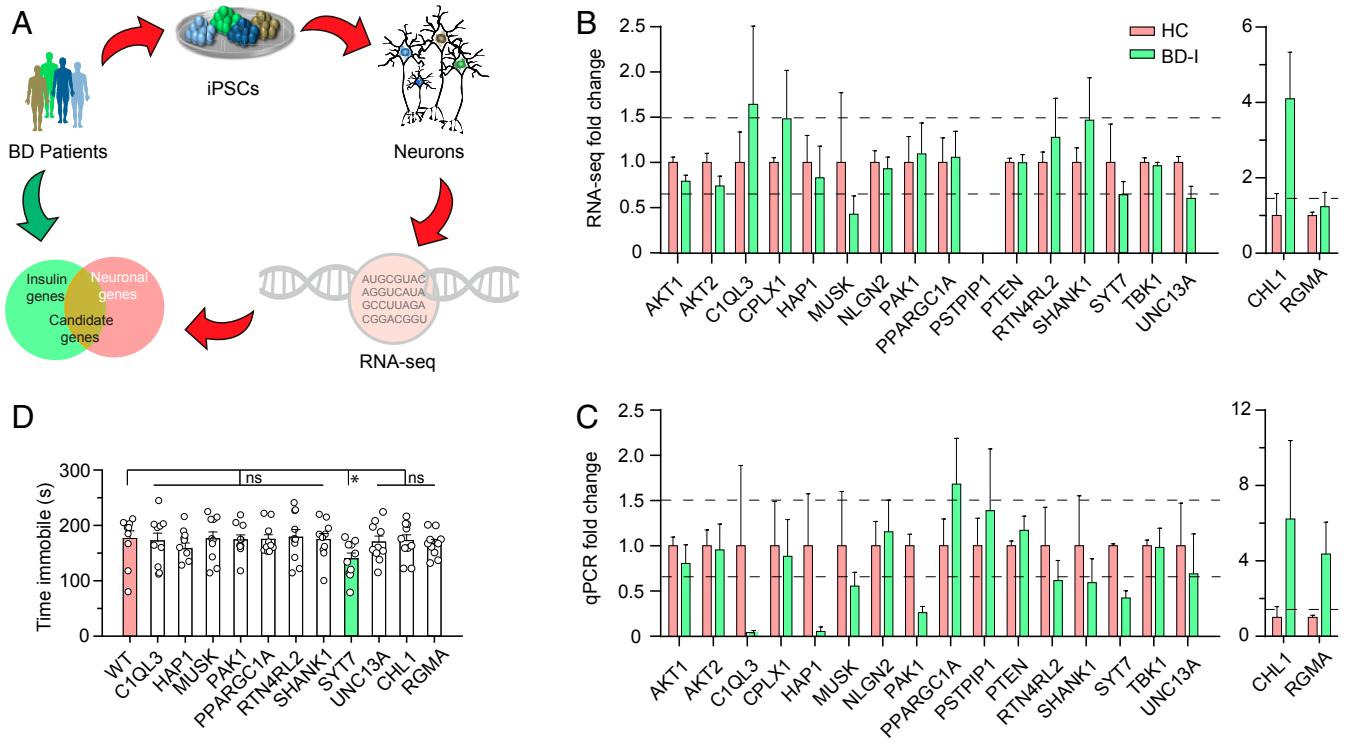

Fig. 1. Identification of Syt7 as a candidate risk factor for behavioral abnormalities. (*A*) Diagram showing the selection of candidate genes using comparative analysis between genes involved in insulin metabolism and neuronal function. (*B* and *C*) RNA-seq (*B*) and qRT-PCR (*C*) analyses of 18 candidate genes in the DG-like neurons studied by Mertens et al. (27). Healthy control (HC), $n = 4$ subjects; type-I bipolar disorder (BD-I), $n = 6$. (*D*) Bar graph showing the immobility time of mice with candidate gene KD in the FST. $n = 10$. Student's t test. $^*P < 0.05$, ns, not significant; error bars, SEM.

the Syt7 KD mice showed a significantly increased moving distance compared to the WT control animals; moreover, the Syt7 KD mice showed an obviously shorter duration in the central area of the field (*SI Appendix*, Fig. S1 *A* and *B*). Therefore, we considered Syt7 to be a candidate risk factor for behavioral abnormalities.

Syt7 Deficiency Induces Behavioral Fluctuations in Mice. To systematically investigate the role of Syt7 in neuropsychiatric-like behaviors, we first verified the Syt7 defects in different subpopulations of BD patients. We separately investigated the iPSC-derived neurons of lithium-responsive (LR) and nonresponsive (NR) patients recruited in two different studies (27, 28). In the two cohorts, the LR and NR neurons both showed an attenuated expression of Syt7 compared to the healthy controls, as evidenced by the results of qRT-PCR and immunoblot analyses (Fig. 2 *A*–*C*).

We then examined the FST performance of Syt7 KO mice (29), which showed energy metabolic abnormalities (*SI Appendix*, Fig. S2). We found that, compared to their WT siblings, nearly 30% of the Syt7 KO mice showed a shorter immobility time in both the dark (Zeitgeber time [ZT] 12–24) and the light (ZT 0–12) phases. Interestingly, more than 60% of the KO animals showed a behavioral fluctuation phenotype with a shorter immobility time in the dark phase and a longer time in the light phase (Fig. 2*D*). Our following behavioral experiments in Syt7 KO mice focused on those showing the day-night swing phenotype. We analyzed the duration of immobility during the tail suspension (TS) test and found that, compared to the WT animals, the Syt7 KO mice showed a significantly shorter immobility time in the dark phase and a longer one in the light phase (Fig. 2*E*). To overcome the concern that the FST/TS approaches might not represent a full spectrum of human diseases, we carried out learned helplessness (LH) and sucrose preference tests (SPT), which indicate the extent of stress and anhedonia, respectively. Compared to the WT mice, in the dark phase, the Syt7 KO mice showed fewer escape

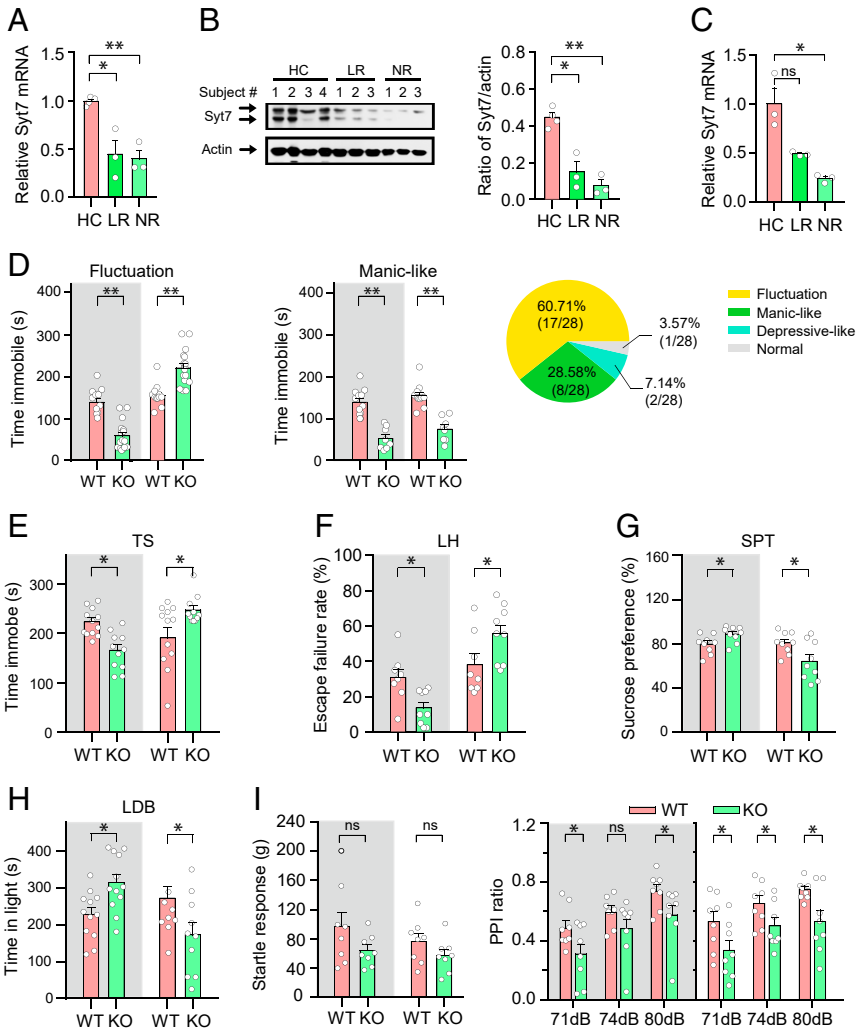

Fig. 2. Insufficient Syt7 expression in patient iPSC-derived neurons and Syt7 deficiency-induced behavioral deficits in mice. (*A* and *B*) qRT-PCR (*A*) and immunoblot (*B*; *Left*, images; *Right*, quantification) analyses of Syt7 in the DG-like neurons of lithium responsive (LR) and nonresponsive (NR) patients studied by Mertens et al. (27). Healthy control (HC), $n = 4$ subjects; LR, $n = 3$; NR, $n = 3$. (*C*) qRT-PCR analysis showing Syt7 expression in the DG-like neurons of LR and NR patients studied by Stern et al. (28). HC, $n = 3$ subjects; LR, $n = 3$; NR, $n = 3$. (*D*) The immobility time of Syt7 KO mice in the FST during the dark and light phases. (*Left*) Summary of Syt7 KO mice showing diurnal fluctuations of immobility time. Gray background, dark phase; white background, light phase. (*Center*) Syt7 KO mice persistently showing a shorter immobility time. (*Right*) Ratio of Syt7 KO mice showing different phenotypes. $n = 28$. (*E*) The immotility of Syt7 KO mice in the TS. $n = 12$. (*F*) The escape failure rate of mice in the LH test. $n = 8$. (*G*) The sucrose preference ratio in the SPT. $n = 8$. (*H*) The duration that mice stayed in the light in a LDB test. Dark, $n = 10$; light, $n = 12$. (*I*) Summary of baseline startle response to auditory-evoked startle stimulus (120 dB) (*Left*) and performance on the PPI test (*Right*). $n = 8$. Student's *t* test. $^*P < 0.05$; $^{**}P < 0.001$; ns, not significant; error bars, SEM.

failures in the LH test and less anhedonia in the SPT, whereas in the light phase, the Syt7 KO animals always showed the reverse performance on these tests (Fig. 2 *F* and *G*). Next, we performed a light/dark box (LDB) test to investigate the anxiety-like behaviors of the Syt7 KO mice. The results indicated that, compared to the WT mice, the Syt7 KO animals showed reduced anxiety in the dark phase but increased anxiety in the light phase (Fig. 2*H*), which is consistent with previous observations in animal models of mood disorders (30). To investigate whether these behavioral abnormalities appeared in an occasional manner, we monitored the locomotor activity of the animals over a 24-h period using the OFT (*SI Appendix*, Fig. S1 *C* and *D*). The results indicated that compared to the WT control group, the locomotor activity of the Syt7 KO mice was increased in the dark phase and decreased in the light phase; moreover, the deviation persisted throughout the dark and light periods, indicating a persistence of the behavioral fluctuation abnormalities. Consistent with the behavioral phenotype, the energy metabolic abnormalities of the Syt7 KO mice also showed a bipolar-like fluctuation pattern (*SI Appendix*, Fig. S2 *C* and *D*). As all these investigations revealed a day-light fluctuation pattern, we tested the circadian rhythm of the Syt7 KO mice, and found that a majority of the animals could exhibit a disorganized circadian rhythm (*SI Appendix*, Fig. S1*E*). In addition, we investigated the psychosis-like behaviors in the Syt7 KO mice using the prepulse inhibition (PPI) paradigm. Compared to the WT mice, the Syt7 KO mice showed a similar acoustic startle response but a significantly reduced PPI ratio regardless of the light condition (Fig. 2*I*).

Together, our results indicated that the Syt7 deficits in iPSC-derived neurons appeared in both the LR and NR patients recruited in two studies; moreover, the Syt7 KO mice showed behavioral abnormalities, a majority of which featured bipolar-like behavioral fluctuations during the dark/light cycle.

Treatment of Syt7 KO Mice with Mood Stabilizing Drugs. To further verify the aberrant behaviors in the Syt7 KO mice, we tested the efficacy of two drugs commonly used in BD, namely olanzapine and lithium, on the behavioral abnormalities of the Syt7 KO mice.

We first treated the Syt7 KO mice with a dose gradient of olanzapine, including 0.2, 0.5, and 1.0 mg/kg. The results of the FST in the Syt7 KO mice revealed that, compared to the nontreated Syt7 KO mice, the middle-dose olanzapine treatment was sufficient to reverse the shortening of the immobility time in the dark phase; moreover, the high-dose treatment elongated the immobility time in the light phase (Fig. 3 *A* and *B*). We noted that the low-dose olanzapine treatment reduced the immobility of the Syt7 KO mice in the light phase (Fig. 3*B*), which was distinct from the outcome of higher doses. Although the reason is unknown, it might be consistent with clinical reports that olanzapine could have antidepressant effects during the treatment of bipolar depression (31). We then tested the efficacy of the high-dose olanzapine treatment (1.0 mg/kg) on the behavioral abnormalities of the Syt7 KO mice using the LH/SPT/LDB paradigms. The results indicated that in both the dark and light phases, the high-dose olanzapine treatment significantly increased the LH escape failure rate, decreased the sucrose preference ratio, and reduced the LDB time-in-light of the Syt7 KO mice compared to the nontreated KO animals (Fig. 3 *C*–*E*). In addition, the WT mice treated with olanzapine showed similar outcomes as the Syt7 KO mice.

We next tested the effects of lithium, a drug that has been widely used for clinical treatment of BD, on the behavioral abnormalities of the Syt7 KO mice. In both the WT and the Syt7 KO mice, lithium carbonate (Li_2CO_3, 30 mg/kg) treatment did not induce any significant changes in the FST immobility time in the dark or light phase (Fig. 3*F*). However, in the LH and SPT experiments, the lithium-treated WT and Syt7 KO mice showed an increased escape failure rate and a decreased sucrose preference ratio in the dark and light phases compared to the nontreated controls (Fig. 3 *G* and *H*). Furthermore, in the LDB test, the lithium treatment did not affect the WT mice, whereas it obviously reduced the time in light in the Syt7 KO mice in the dark and light phases compared to the nontreated Syt7 KO animals (Fig. 3*I*).

Together, our results indicated that the clinical drug treatments had significant effects on the behavioral abnormalities of the Syt7 KO mice.

Evaluation of Syt7 Expression in Patient Plasma Samples. Finally, to investigate whether the Syt7 defects shown by the iPSC-derived neurons existed in BD patients, we analyzed the mRNA level of Syt7 in the plasma samples of BD patients. We collected blood samples of 20 BD patients and 11 age- and gender-matched healthy controls and separated the plasma from the blood cells (Fig. 4*A* and *SI Appendix*, Table S1). We then carried out qRT-PCR analysis to evaluate the Syt7 mRNA level in the plasma samples. The results showed that, compared to the healthy control group, the BD patient group showed a significant reduction in Syt7 mRNA level (Fig. 4*B*), indicating that the Syt7 defects detected in the iPSC-derived neurons indeed existed in a subpopulation of BD patients.

We then categorized the patients into subgroups based on age, gender, disease course, and severity. In general, most subgroups of patients showed a trend of decline in the plasma Syt7 mRNA level compared to their matched healthy controls (*SI Appendix*, Fig. S3). We note that the patients >30 y old did not show a substantial attenuation in the plasma Syt7 mRNA level compared to the controls (*SI Appendix*, Fig. S3*F*). Although the sample size was relatively low, this result indicated that the Syt7 defects could be more prominent in the subpopulation of young adult patients. We further analyzed the patients grouped according to disease subtype, family BD history, drugs treatment, and presence of psychosis. We found that, compared to the healthy controls, both BD-I and BD-II subgroups showed a significant reduction in the plasma Syt7 mRNA level (Fig. 4*C*). Furthermore, compared to the healthy subjects, the patients without psychosis or family BD history showed significant reductions in Syt7 mRNA level, and those with psychotic symptoms or family BD history also showed a decline trend in Syt7 mRNA (Fig. 4 *D* and *E*). Importantly, the subgroup of untreated patients, although the sample size was small, showed a remarkable decrease in Syt7 mRNA level, whereas the drug-treated subgroup showed a slightly restored Syt7 mRNA expression, although it was still obviously lower than that of the healthy control group (Fig. 4*F*).

In addition, we have also investigated the Syt7 mRNA level in the blood cells of the healthy control subjects and BD patients. The results indicated that consistent with the plasma tests, the blood cells of the BD patients showed a significantly reduced Syt7 mRNA level compared to the healthy control group (*SI Appendix*, Fig. S3*G*).

Discussion

Despite current progress in the identification of genetic variants in BD patients, we have not yet delineated the pathogenesis of the disease, probably due to its complex multigenic origin. To overcome the shortcoming of genetic rodent models with only one or two genes modified and the time-consuming cross-mating of multiple transgenic strains, patient iPSC models have been employed, as a cell platform closer to the disease, to explore the molecular and cellular deficits fundamental to the pathogenesis of BD. Previously, we demonstrated that the hippocampal DG-like neurons derived from the iPSCs of six BD-I patients showed very similar gene expression profiles (27), which indicated that, regardless of the various genetic deficiencies the six patients might carry, these subjects probably shared common molecular and cellular deficits that are crucial for the induction of the homologous mood abnormalities. Given the strong disease inheritance within the pedigree, it is possible that, among the involved molecules and

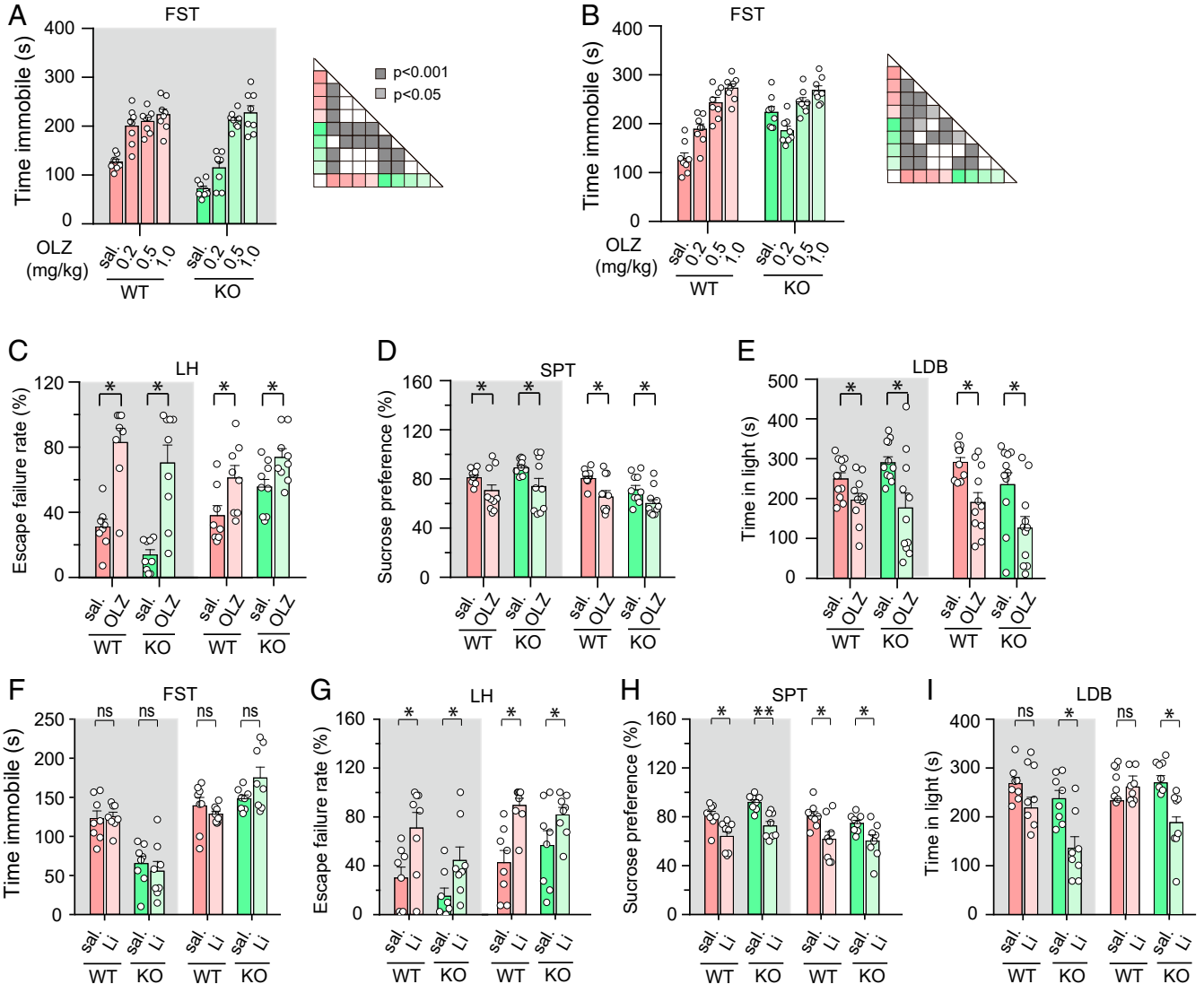

Fig. 3. Effects of olanzapine (OLZ) and lithium on the behavioral abnormalities of Syt7 KO mice. (*A* and *B*) Effects of OLZ i.p. injection (0.2–1.0 mg/kg) on FST immobility of Syt7 KO mice in the dark (*A*) and light (*B*) phases. ANOVA test. (*C–E*) Effects of high dose OLZ treatment (1.0 mg/kg) on LH escape failure rate (*C*), SPT sucrose preference ratio (*D*) and LDB time in light (*E*) of Syt7 KO mice. (*F–I*) Effects of Li_2CO_3 i.p. injection (30 mg/kg) on FST immobility time (*F*), LH escape failure rate (*G*), SPT sucrose preference ratio (*H*), and LDB time in light (*I*). $n = 8$ for all experiments. Student's *t* test. $^*P < 0.05$; ns, not significant; error bars, SEM.

pathways, some might play an essential role in the etiology of BD, whereas others are auxiliary or secondary, and thus the disease can occur in a majority of the offspring as the deficits in such a key molecular mechanism can be stably inherited. Although changes in the molecules may cause alterations at the molecular, cellular, and neural circuit levels that are essential for the pathogenesis of the disease, they are not required to have variants in the patients.

To efficiently identify the molecules that contribute to the behavioral abnormalities in patients, we carried out a preliminary test on the expression and function of those genes involved in the comorbidities of BD in the patient iPSC-derived neurons. One major comorbidity of BD is the insulin/glucose metabolic syndrome, which affects more than 40% of BD patients (7–9). We hypothesized that the deficits of the key molecular pathway in the brain induce behavioral symptoms, whereas they can generate insulin metabolic symptoms if they occur in the islets, which might be one reason why the two diseases are comorbid. Compared to BD, the research on insulin-related metabolic abnormalities has made much greater progress in the past decades, providing us with an abundant resource of candidate molecules for investigation in patient iPSC-derived neurons (Fig. 1*A*).

In the present study, we searched public databases and determined <20 candidate genes that were likely to be associated with both the insulin metabolic and the neuronal signaling processes. Our experiments demonstrated that, among these genes, Syt7 appeared to play a key role in the generation of manic-like and depressive-like behavioral abnormalities in mice. At present, there is no report of genome-wide association study that the single nucleotide polymorphisms (SNPs) of Syt7 have been identified in BD patients. However, in the plasma samples of BD patients, the mRNA level of Syt7 also showed an obvious trend of decline compared to healthy controls. We noted that not all patients showed reduced plasma Syt7 expression compared to the average level of healthy control subjects. Although the Syt7 mRNA level in the patient blood might not accurately reflect the expression of Syt7 in the brain, it is possible that the key molecule or pathway differs in different subpopulations of patients, which, however, might still cause identical functional consequences to induce analogous behavioral abnormalities.

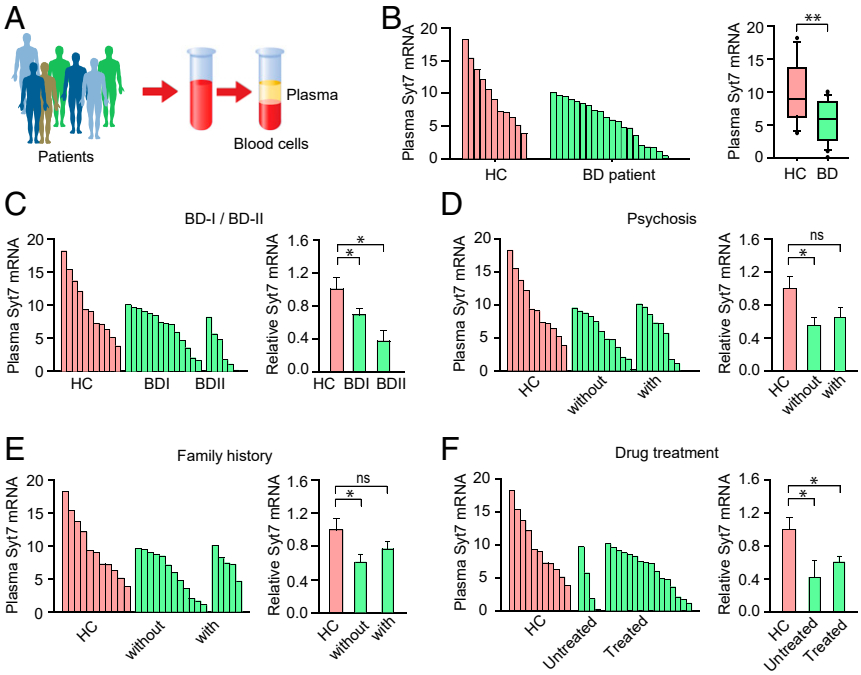

Fig. 4. Syt7 mRNA level in BD patient plasma samples. (*A*) Diagram showing the analysis of Syt7 mRNA in plasma samples of BD patients. (*B*) Quantitative analysis of Syt7 mRNA in the plasma of 20 BD patients and 11 healthy controls. (*C*) Syt7 mRNA level in BD-I ($n = 11$) and BD-II ($n = 5$) subgroups. (*D*) Syt7 mRNA level in patients with ($n = 7$) and without ($n = 10$) complications. (*E*) Syt7 mRNA level in patients with ($n = 5$) and without ($n = 9$) family BD history. (*F*) Syt7 mRNA level in treated ($n = 14$) and untreated ($n = 3$) patients. Student's *t* test. $*P < 0.05$; $**P < 0.001$; error bars, SEM.

One important question is how the multiple or diverse genetic variants in a subpopulation of patients can functionally converge on a single molecular mechanism like the Syt7-involved pathway to induce similar downstream pathogenic consequences. One possible mechanism is that the susceptible gene itself is involved in some element within the mechanistic pathway. For instance, the variants of two susceptible genes, DBP and CLOCK, might disturb the circadian rhythm (32, 33). In an alternative explanation, cis-regulatory chromatin contact might play a role in the contribution of genetic variants to the pathogenesis of BD. At present, little evidence is available to directly show a linkage between the SNPs and those genes involved in the key molecular pathway in BD patients. This is not only due to the lack of knowledge about the molecular mechanisms underlying the mood abnormalities but is also attributable to our poor understanding of the interactions between genetic variants and their cognate genes over long genomic distances. Recently, it has been suggested that the SNPs of the obesity-related gene FTO target the IRX3 and IRX5 genes over long distances but not the FTO itself (34, 35). This finding implies that the genetic variants in BD patients might also act through regulating the expression of other genes far from the loci of the variants, rather than altering the nearest gene. Hence, one possible reason why many genetic rodent models have failed to show the symptoms of BD could be the differences in chromatin structure between humans and rodents. In this case, the iPSC model of BD patients would be an appropriate platform to study the contribution of long-distance DNA–DNA interactions to the pathogenesis of BD. We consider that this possibility might also be the case for other mental disorders such as schizophrenia and autism.

Another important consideration is the role of circadian rhythm in BD. Previously, circadian genes such as CLOCK and DBP were identified as susceptible genes for BD (36–38). In recent years, a large amount of clinical evidence has suggested that circadian rhythm dysfunction is a trait marker of BD and probably governs the onset and relapse of BD episodes; moreover, the duration of the BD episodes is likely determined by the combined effects of endogenous dysfunction and external perturbations of the circadian rhythm (39–41). In the present study, although some Syt7 KO mice showed persistent manic-like or depressive-like behavioral abnormalities, a majority of the KO mice showed a diurnal pattern of behavioral fluctuations, probably because only endogenous circadian-based dysfunctions acted in these animals. In the future, it would be interesting to investigate whether the episodes of these mice can be extended through applying some external circadian perturbation approaches.

In summary, we demonstrated that Syt7 showed an attenuated expression in patient iPSC-derived neurons and plasma samples and that Syt7 deficiency induced circadian-based fluctuation of neuropsychiatric-like behaviors in mice. We therefore conclude that Syt7 is likely a key factor for behavioral fluctuations in mice, and deficits in Syt7 might make a crucial contribution to the behavioral abnormalities in a subpopulation of BD patients through coactions with other biological and environmental factors.

Materials and Methods

Clinical Patient Information and Blood Samples. The clinical information of the patients used for the iPSC experiments has been described previously (27, 28). Of the six patients investigated by Stern et al. (28), one suffered type 2 diabetes and the other five did not show symptoms of diabetes or metabolic syndrome. As for the six patients investigated by Mertens et al. (27), the metabolic information of the patients is unknown.

All human donor blood samples described here were obtained from subjects who had given informed consent, and all procedures were approved by the ethical committee of the Affiliated Brain Hospital of Guangzhou Medical University (Guangzhou Huiai Hospital), China. Patients were selected based on diagnosed as BD, which was determined/diagnosed by trained postgraduates or psychiatrists by using the Diagnostic and Statistical Manual of Mental Disorders, Fifth Edition (DSM-5). All individuals were of Han Chinese ethnicity. Self-reported information on gender and prior history of diseases is given in *SI Appendix*, Table S1. Of the 20 patients, 10 had shown symptoms of metabolic syndrome.

Blood was collected from healthy and BD donors on an empty stomach in ethylenediaminetetraacetic acid (EDTA) tubes (BD Biosciences 366643). The blood was initially centrifuged at 3,000 × *g* for 10 min to separate the

plasma and blood cells. The supernatant was carefully removed and centrifuged again at 2,500 × *g* for 15 min to separate plasma and platelets. For serum or plasma, total RNA was extracted from 100 μL of the sample using the miRNeasy kit (Qiagen). The extracted RNA was assessed for quality and quantity with NanoDrop 1000 spectrophotometer (Thermo Scientific). The cDNA was then generated using AccuRT Genomic DNA Removal Kit (Abm, Canada). qPCR was performed using SYBR Green.

Lentivirus Preparation and Infection. The shRNAs were provided by The RNAi Consortium library. Lentiviral particles were generated and collected as previously described (42). Briefly, to generate lentiviral particles, HEK 293FT cells cultured with Dulbecco's modified Eagle medium (DMEM) in 10% fetal bovine serum (FBS) and 2 mM glutamax (Life Technologies) were cotransfected with virus packaging vectors using PEI (Polysciences). After 3 d, the supernatant of culture medium was harvested and filtered with a 0.22-μm polyvinylidene fluoride (PVDF) filter (Millipore). Virus particles were collected by ultracentrifugation at 25,000 rpm in a P28S rotor (Hitachi) in a final volume of 100 μL. The titer of the lentivirus used for in vivo stereotactic injection experiments was concentrated to at least 1.0×10^{10} infectious units (IU) per milliliter.

Differentiation of iPSCs into DG-like Neurons. The forebrain neural progenitor cells (NPCs) derived from BD patients and healthy subjects were characterized as previously described (27, 28). Information about the approving committee, informed consent, and clinical trial registration number of the iPSC studies are described in the original articles (27, 28). To obtain hippocampal DG-like neurons, NPCs were differentiated in DMEM/F12 supplemented with N2 (Life Technologies), B27 (Life Technologies), 20 ng/mL brain-derived neurotrophic factor (BDNF) (Peprotech), 1 mM dibutyrl-cyclicAMP (Sigma), 200 nM ascorbic acid (Sigma), 1 μg/mL Laminin, and 620 ng/mL Wnt3a (R&D) for 3 to 4 wk. Wnt3a was removed after 3 wk. All cells used in the present study were verified as mycoplasma contamination free.

Behavioral Assays. Syt7 KO mice were kindly provided by E. R. Chapman (University of Wisconsin, Madison, WI) with permission from N. W. Andrews (University of Maryland, College Park, MD). All of the animal experiments were conducted using 3- to 6-mo-old male mice under the guidance and approval of the Institutional Animal Care & Use Committee of Tsinghua University and the Animal Welfare and Ethics Committee of Tsinghua University (Approval ID: 15-YJ2). WT siblings of similar age were used as a control for the Syt7 KO mice. Different groups of mice were used for dark-phase and light-phase testing. Activity was recorded by a suspended digital camera and analyzed by EthoVision XT 11.5 (Noldus) after 30 min habituation in the test room (600 lx) in light/dark box test. The same parameter setting for the definition of each behavior was applied for all of the mice tested in different behavior tests. For the drug treatment experiment, unless specified, the drug solutions or vehicle control were injected or infused 30 min before the behavioral tests at the indicated dose. Animals that accidentally died during the study were included in analysis for all completed tests. The data were analyzed by EthoVision XT 11.5 software (Noldus).

Locomotor activity. The 24-h locomotor activity was measured using the 16-chamber TSE phenoMaster/LabMaster (TSE Systems) after the drug or control vesicle solution was administered. Consecutive adjacent infrared beam breaks in either the *x* or *y* axes were scored as an activity count, and a tally was recorded every 6 min. In regular open field test, an open field arena (50 cm × 50 cm × 40 cm) was used to measure animal locomotor activity. Mice were placed in the center of the arena and allowed to freely explore it for 10 min with dim light.

Circadian rhythm. To assay the circadian rhythm, mice were held on a 12:12 light/dark cycle for 2–8 d in TSE with food and water and with the temperature at 21 ± 2 °C. Mice were then released into constant dark for 16 d.

PPI. Mice were placed in a test chamber (San Diego Instruments) and habituated for 15 min with 68 dB background white noise that continued throughout the session. On the following day, subjects received a block of five 40-ms startle pulses of 120 dB and then received 10 blocks of trials each to measure PPI, followed by another six startle pulses. Each block of trials consisted of eight trial types (i. no stimulus; ii. one 40 ms startle stimulus; iii–v. three different prepulse sounds [20 ms 74, 78, 82 dB] alone; vi–viii. three prepulse sounds 100 ms before the startle stimulus) presented in pseudo-random order across blocks. The interval between each trial type was 10–20 s. The maximum amplitude was recorded for every trial. PPI was calculated as: 1 − startle amplitude in the prepulse trial/startle amplitude in the startle alone trial.

FST. Animals were individually introduced to a cylinder (20 cm diameter × 30 cm height) filled with 15 cm of water (23 ± 1 °C) and swam for 6 min under normal light. Immobility time was defined as the time when animals remained floating or motionless that necessary to keep balance in the water. Data acquisition and analyses were carried out by trained individuals blind to the genotype and treatment during the test.

TS. Animals were individually hung by their tails from a bar 40 cm from the ground for 6 min under normal light. The animals' movements were recorded by a video. Immobility was scored by a trained observer blinded to genotypes and treatments. The behavior rated was immobility: hanging by the tail without engaging in any active upward movements of the entire body.

SPT. Mice were held on a 12:12 light/dark cycle with food and water and with the temperature at 21 ± 2 °C. The test began at the dark phase of animal activity. Mice were placed individually in a chamber equipped with two bottles on opposite walls throughout the experiment (36 h). One bottle was filled with 2% sucrose solution, and the other bottle was filled with water. The mice were habituated in the chamber for 12 h. Then the bottles of sucrose solution and water were weighed at 12-, 24-, and 36-h time points to determine the sucrose and water intake in the dark and light phases. To avoid any confounding effect of side preference, the position of the sucrose and water bottles was exchanged every 6 h. Sucrose preferences were calculated as follows: sucrose consumed/(sucrose consumed + water consumed).

LH. The LH model consisted of three different phases: inescapable shock training, LH screening, and the test. Mice were placed in one chamber of two-chamber shuttle boxes (MedAssociates) for a 5-min adaptation period before the test. During the inescapable shock training phase (days 1–3), the mice received 120 inescapable foot-shocks (0.45 mA, 15-s duration, randomized average inter-shock interval 45 s) with the door closed between the two chambers of the shuttle boxes each day. For the LH screening phase (day 4), the door was raised at the onset of the shock (0.45 mA), and the shock ended either when the mouse stepped through to the other side of the shuttle boxes or after 3 s. Mice that had more than five escape failures developed helplessness behavior during the 10 screening shocks. On the test day, the animals were placed in the shuttle boxes and 0.45-mA shocks were delivered concomitantly with door opening for the first five trials, followed by a 2-s delay for the next 40 trials and intertrial intervals were randomized at an average of 30 s. The shock was terminated either when the animal crossed over to the second chamber or after 24 s. Latency to step through the door and the number of escape failures were recorded for the last 40 trials by automated software (MED-PC IV).

LDB test. Mice were placed singly in the dark side of the light/dark box apparatus and allowed to move freely for 10 min; the time spent in the light box was analyzed.

Resting metabolic rate. Resting metabolic rate (RMR) was measured using an open-flow respiratory system (Sable, FoxBox). Individual mice were transferred into transparent plastic chambers (volume 860 mL, 11 × 11 × 7.6 cm) housed inside a constant-temperature incubator (Yiheng Model LRH-250) set to 30 ± 0.5 °C. Fresh air from outside was dried using a column filled with DRIERITE desiccant (W. A. Hammond Drierite), then warmed to 30 ± 0.5 °C by passage through a copper coil inside the cabinet, and pumped through the chamber at a flow rate of 600–800 mL/min. Subsequently, air leaving the animal chamber was dried using a nonchemical gas drier (Sable, ND-2), then passed through a gas analyzer at the rate of 100 mL/min. Each measurement lasted 3 h, with data recorded every 15 s. RMR was quantified as the oxygen consumption (VO_2; mL/min) calculated as the average of 5-min stable lowest values. Body mass was recorded before the measurement.

Immunoblot Analysis. Neurons were lysed in radioimmunoprecipitation assay (RIPA) buffer with a protease inhibitor mixture (Roche). Lysates were centrifuged at 2,000 × *g* for 10 min, and equal amounts of supernatants were loaded per lane and resolved by SDS/PAGE. The blots were developed using an electrochemiluminescence (ECL) kit (Pierce). Primary antibodies include a rabbit polyclonal antibody specific for Syt7 (1:200, Synaptic Systems, no. 105173) and a mouse monoclonal antibody specific for β-actin (1:5,000, Abcam, no. ab6276). Protein levels were analyzed with ImageJ software (NIH).

qRT-PCR. Total cellular RNA was extracted using TRIzol (Life Technologies) according to the manufacturer's instructions, and reverse transcription was performed using SuperScript III Reverse Transcription Kit (Life Technologies). qRT-PCR was performed with SYBR green supermix (Bio-Rad) on a Bio-Rad CFX96 thermal cycler, and the results were analyzed using the ΔΔCT method. The primer sequences are listed in *SI Appendix*, Table S2.

Statistical Analysis. Data are shown as mean values ± SEM. Two-way ANOVA analysis was used for experiments in Fig. 3 *A* and *B*; two-tailed unpaired Student's *t* test was used for all other experiments. The analysis approaches have been justified as appropriate by previous biological studies, and all data met the criteria of normal distribution. The statistical data for

all experiments are listed in *SI Appendix*, Table S3. Statistical significance was evaluated at $P < 0.05$.

Data Availability. All of the data, associated protocols, and materials for this study are available within the paper and in *SI Appendix*.

ACKNOWLEDGMENTS. We thank Drs. Xuan Huang, Anbang Dai, and Shan Sun (Tsinghua University) for technical help, and all members of the J.Y. laboratory for assistance. This work was supported by National Key R&D Program of China Grant No. 2016YFA0101900; National Natural Science Foundation of China Grants 31830038, 31771482, and 81771466; Beijing Municipal Science & Technology Commission Grant Z181100001518001; the Open Project of State Key Laboratory of Membrane Biology; and National Institutes of Health Grants U19MH106434 and U01MH106882. The content is solely the responsibility of the authors and does not necessarily represent the official views of the NIH. Additional support was provided from the JPB Foundation, The Engman Foundation, the Leona M. and Harry B. Helmsley Charitable Trust, Annette Merle-Smith, and the Mathers Foundation.

1. N. Craddock, P. Sklar, Genetics of bipolar disorder. *Lancet* **381**, 1654–1662 (2013).
2. K. Roybal *et al*., Mania-like behavior induced by disruption of CLOCK. *Proc. Natl. Acad. Sci. U.S.A.* **104**, 6406–6411 (2007).
3. J. W. Young, B. L. Henry, M. A. Geyer, Predictive animal models of mania: Hits, misses and future directions. *Br. J. Pharmacol.* **164**, 1263–1284 (2011).
4. I. D. Neumann *et al*., Animal models of depression and anxiety: What do they tell us about human condition? *Prog. Neuropsychopharmacol. Biol. Psychiatry* **35**, 1357–1375 (2011).
5. A. N. Sharma *et al*., Modeling mania in preclinical settings: A comprehensive review. *Prog. Neuropsychopharmacol. Biol. Psychiatry* **66**, 22–34 (2016).
6. Y. Kim, R. Santos, F. H. Gage, M. C. Marchetto, Molecular mechanisms of bipolar disorder: Progress made and future challenges. *Front. Cell. Neurosci.* **11**, 30 (2017).
7. M. Ruzickova, C. Slaney, J. Garnham, M. Alda, Clinical features of bipolar disorder with and without comorbid diabetes mellitus. *Can. J. Psychiatry* **48**, 458–461 (2003).
8. T. Hajek, R. McIntyre, M. Alda, Bipolar disorders, type 2 diabetes mellitus, and the brain. *Curr. Opin. Psychiatry* **29**, 1–6 (2016).
9. A. Wysokiński, D. Strzelecki, I. Kłoszewska, Levels of triglycerides, cholesterol, LDL, HDL and glucose in patients with schizophrenia, unipolar depression and bipolar disorder. *Diabetes Metab. Syndr.* **9**, 168–176 (2015).
10. F. Talbot, A. Nouwen, A review of the relationship between depression and diabetes in adults: Is there a link? *Diabetes Care* **23**, 1556–1562 (2000).
11. C. N. Egbujo, D. Sinclair, C. G. Hahn, Dysregulations of synaptic vesicle trafficking in schizophrenia. *Curr. Psychiatry Rep.* **18**, 77 (2016).
12. R. B. Cupertino *et al*., SNARE complex in developmental psychiatry: Neurotransmitter exocytosis and beyond. *J. Neural. Transm. (Vienna)* **123**, 867–883 (2016).
13. E. T. Kavalali, L. M. Monteggia, How does ketamine elicit a rapid antidepressant response? *Curr. Opin. Pharmacol.* **20**, 35–39 (2015).
14. M. Ayalew *et al*., Convergent functional genomics of schizophrenia: From comprehensive understanding to genetic risk prediction. *Mol. Psychiatry* **17**, 887–905 (2012).
15. N. Li *et al*., mTOR-dependent synapse formation underlies the rapid antidepressant effects of NMDA antagonists. *Science* **329**, 959–964 (2010).
16. A. E. Autry *et al*., NMDA receptor blockade at rest triggers rapid behavioural antidepressant responses. *Nature* **475**, 91–95 (2011).
17. O. H. Miller *et al*., GluN2B-containing NMDA receptors regulate depression-like behavior and are critical for the rapid antidepressant actions of ketamine. *eLife* **3**, e03581 (2014).
18. C. Kiselycznyk, P. Svenningsson, E. Delpire, A. Holmes, Genetic, pharmacological and lesion analyses reveal a selective role for corticohippocampal GLUN2B in a novel repeated swim stress paradigm. *Neuroscience* **193**, 259–268 (2011).
19. H. Wen *et al*., Distinct roles for two synaptotagmin isoforms in synchronous and asynchronous transmitter release at zebrafish neuromuscular junction. *Proc. Natl. Acad. Sci. U.S.A.* **107**, 13906–13911 (2010).
20. T. Bacaj *et al*., Synaptotagmin-1 and synaptotagmin-7 trigger synchronous and asynchronous phases of neurotransmitter release. *Neuron* **80**, 947–959 (2013).
21. H. Liu *et al*., Synaptotagmin 7 functions as a Ca2+-sensor for synaptic vesicle replenishment. *eLife* **3**, e01524 (2014).
22. S. L. Jackman, J. Turecek, J. E. Belinsky, W. G. Regehr, The calcium sensor synaptotagmin 7 is required for synaptic facilitation. *Nature* **529**, 88–91 (2016).
23. D. Wu *et al*., Postsynaptic synaptotagmins mediate AMPA receptor exocytosis during LTP. *Nature* **544**, 316–321 (2017).
24. Y. C. Li, N. L. Chanaday, W. Xu, E. T. Kavalali, Synaptotagmin-1- and synaptotagmin-7-dependent fusion mechanisms target synaptic vesicles to kinetically distinct endocytic pathways. *Neuron* **93**, 616–631.e3 (2017).
25. N. Gustavsson *et al*., Impaired insulin secretion and glucose intolerance in synaptotagmin-7 null mutant mice. *Proc. Natl. Acad. Sci. U.S.A.* **105**, 3992–3997 (2008).
26. B. Wu *et al*., Synaptotagmin-7 phosphorylation mediates GLP-1-dependent potentiation of insulin secretion from β-cells. *Proc. Natl. Acad. Sci. U.S.A.* **112**, 9996–10001 (2015).
27. J. Mertens *et al*.; Pharmacogenomics of Bipolar Disorder Study, Differential responses to lithium in hyperexcitable neurons from patients with bipolar disorder. *Nature* **527**, 95–99 (2015).
28. S. Stern *et al*., Neurons derived from patients with bipolar disorder divide into intrinsically different sub-populations of neurons, predicting the patients' responsiveness to lithium. *Mol. Psychiatry* **23**, 1453–1465 (2018).
29. S. Chakrabarti *et al*., Impaired membrane resealing and autoimmune myositis in synaptotagmin VII-deficient mice. *J. Cell Biol.* **162**, 543–549 (2003).
30. R. W. Logan, C. A. McClung, Animal models of bipolar mania: The past, present and future. *Neuroscience* **321**, 163–188 (2016).
31. T. Atkin, N. Nuñez, G. Gobbi, Practitioner review: The effects of atypical antipsychotics and mood stabilisers in the treatment of depressive symptoms in paediatric bipolar disorder. *J. Child Psychol. Psychiatry* **58**, 865–879 (2017).
32. H. Le-Niculescu *et al*., Phenomic, convergent functional genomic, and biomarker studies in a stress-reactive genetic animal model of bipolar disorder and co-morbid alcoholism. *Am. J. Med. Genet. B. Neuropsychiatr. Genet.* **147B**, 134–166 (2008).
33. C. A. McClung *et al*., Regulation of dopaminergic transmission and cocaine reward by the Clock gene. *Proc. Natl. Acad. Sci. U.S.A.* **102**, 9377–9381 (2005).
34. S. Smemo *et al*., Obesity-associated variants within FTO form long-range functional connections with IRX3. *Nature* **507**, 371–375 (2014).
35. M. Claussnitzer *et al*., FTO obesity variant circuitry and adipocyte browning in humans. *N. Engl. J. Med.* **373**, 895–907 (2015).
36. J. Morissette *et al*., Genome-wide search for linkage of bipolar affective disorders in a very large pedigree derived from a homogeneous population in quebec points to a locus of major effect on chromosome 12q23-q24. *Am. J. Med. Genet.* **88**, 567–587 (1999).
37. T. Takao, H. Tachikawa, Y. Kawanishi, K. Mizukami, T. Asada, CLOCK gene T3111C polymorphism is associated with Japanese schizophrenics: A preliminary study. *Eu. Neuropsychopharmacol.* **17**, 273–276 (2007).
38. H. A. Mansour *et al*., Association study of eight circadian genes with bipolar I disorder, schizoaffective disorder and schizophrenia. *Genes Brain Behav.* **5**, 150–157 (2006).
39. L. B. Alloy, T. H. Ng, M. K. Titone, E. M. Boland, Circadian rhythm dysregulation in bipolar spectrum disorders. *Curr. Psychiatry Rep.* **19**, 21 (2017).
40. M. J. McCarthy, D. K. Welsh, Cellular circadian clocks in mood disorders. *J. Biol. Rhythms* **27**, 339–352 (2012).
41. Y. Takaesu *et al*., Circadian rhythm sleep-wake disorders predict shorter time to relapse of mood episodes in euthymic patients with bipolar disorder: A prospective 48-week study. *J. Clin. Psychiatry* **79**, 17m11565 (2018).
42. Y. Zheng *et al*., CRISPR interference-based specific and efficient gene inactivation in the brain. *Nat. Neurosci.* **21**, 447–454 (2018). Erratum in: *Nat. Neurosci.* **21**, 894 (2018).

Supplementary Information for

Synaptotagmin-7 is a key factor for bipolar-like behavioral abnormalities in mice

Wei Shen[a1], Qiu-Wen Wang[a1], Yao-Nan Liu[a1], Maria C. Marchetto[b], Sara Linker[b], Si-Yao Lu[a], Yun Chen[a], Chuihong Liu[c], Chongye Guo[d], Zhikai Xing[d], Wei Shi[e], John R. Kelsoe[f], Martin Alda[g], Hongwei Wang[h], Yi Zhong[i], Sen-Fang Sui[j], Mei Zhao[k], Yiming Yang[l], Shuangli Mi[d], Liping Cao[c], Fred H. Gage[b], and Jun Yao[a]

[a] State Key Laboratory of Membrane Biology, Tsinghua-Peking Center for Life Sciences, IDG/McGovern Institute for Brain Research, School of Life Sciences, Tsinghua University, Beijing 100084, China.
[b] Laboratory of Genetics, The Salk Institute for Biological Studies, La Jolla, CA 92037, USA.
[c] Affiliated Brain Hospital of Guangzhou Medical University, Guangzhou Huiai Hospital, Guangzhou 510370, Guangdong, China.
[d] Key Laboratory of Genomic and Precision Medicine, Beijing Institute of Genomics, Chinese Academy of Sciences, Beijing 100101, China; University of Chinese Academy of Sciences, Beijing, 100049, China.
[e] Beijing Advanced Innovation Center for Big Data-based Precision Medicine, Beihang University, Beijing 100191, China.
[f] Institute for Genomic Medicine, University of California San Diego, La Jolla, CA, 92093, USA.
[g] Department of Psychiatry, Dalhousie University, Halifax, NS, Canada.
[h] Tsinghua-Peking Center for Life Sciences, School of Life Sciences, Tsinghua University, Beijing 100084, China.
[i] Tsinghua-Peking Center for Life Sciences, IDG/McGovern Institute for Brain Research, School of Life Sciences, Tsinghua University, 100084, Beijing, China.
[j] State Key Laboratory of Membrane Biology, Beijing Advanced Innovation Center for Structural Biology, School of Life Sciences, Tsinghua University, Beijing 100084, China.
[k] CAS, Key Lab of Mental Health, Institute of Psychology, Beijing 100101, China; University of Chinese Academy of Sciences, Beijing 101408, China.
[l] School of Linguistic Sciences and Arts, Collaborative Innovation Center for Language Ability, Jiangsu Normal University, Xuzhou 221009, Jiangsu, China.

[1] These authors contributed equally to this study.

Please address correspondence to: Fred H. Gage (gage@salk.edu) or Jun Yao (jyao@mail.tsinghua.edu.cn).

This PDF file includes:

Figure S1 to S3.
Table S1 to S3.

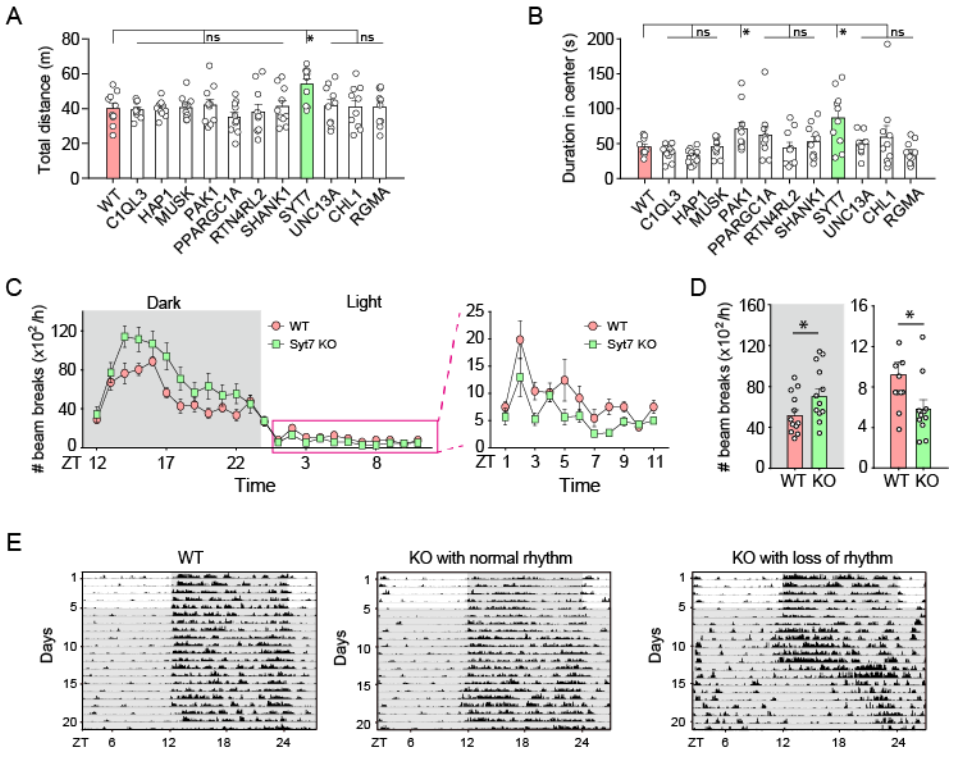

Fig. S1. Locomotor activity and circadian rhythm of Syt7-deficient mice. (**A**) Bar graph showing the total moving distance of mice with candidate gene KD in the open field test (OFT). n = 10. (**B**) The duration of the mice in the center of the open field. (**C**) Summary of locomotor activity of Syt7 KO mice over 24 hours. Right panel, enlarged summary of locomotor activity during the light phase. n = 8. (**D**) Average locomotor activity of Syt7 KO mice in the dark and light phases. n = 8. (**E**) Circadian rhythms of WT (left) and Syt7 KO (middle and right) mice. Of the five Syt7 KO mice, two showed a normal circadian rhythm (middle) and three exhibited similar abnormal circadian rhythms (right). WT, n = 6; Syt7 KO, n = 5. Student's *t*-test. **P* < 0.05; ***P* < 0.001; error bars, s.e.m.

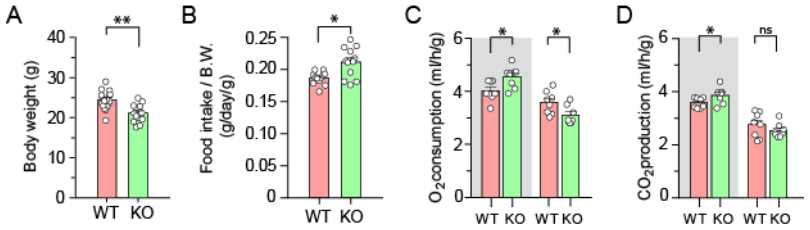

Fig. S2. Metabolic abnormalities of Syt7 KO mice. (**A**) Bar graphs showing the body weight of WT and Syt7 KO mice. WT, n = 17; KO, n = 14. (**B**) Food intake of WT and Syt7 KO mice. n = 12. (**C and D**) Resting metabolic rates of WT and Syt7 KO mice in the dark and light phases, including oxygen consumption (**C**) and CO2 production (**D**). n = 8. Student's *t*-test. **P* < 0.05; ***P* < 0.001; error bars, s.e.m.

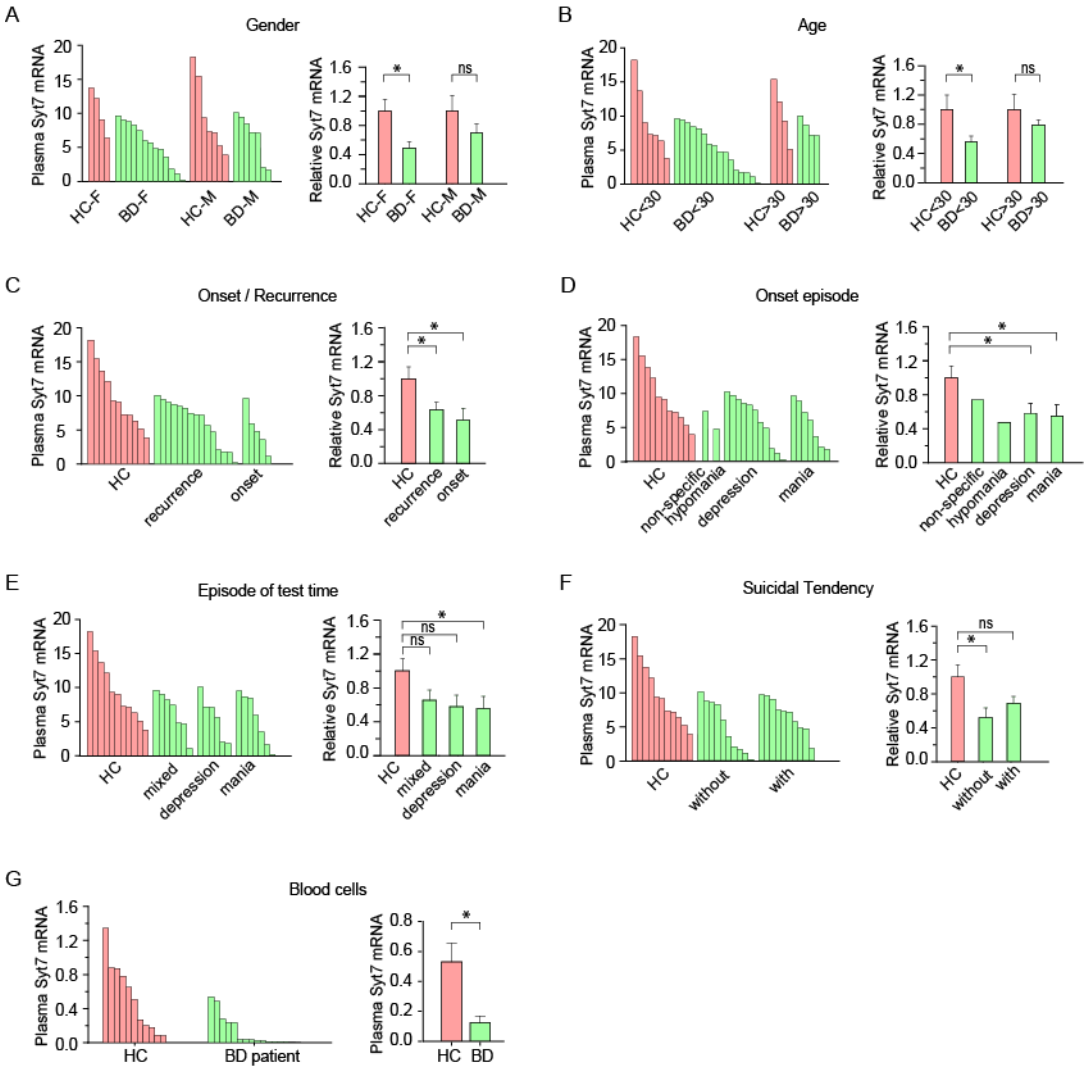

Fig. S3. Syt7 mRNA level in the plasma samples of subgroups of BD patients and in the blood cells of BD patients. (**A**) Syt7 mRNA level in the plasma of female (F) (n = 13) and male (M) (n = 7) patients. HC, healthy control. HC-F, n = 4; HC-M, n = 7. (**B**) Syt7 mRNA level in patients <30 years and >30 years old. HC<30, n = 7; BD<30, n = 16; HC>30, n = 4; BD>30, n = 4. (**C**) Syt7 mRNA level in patients at onset or recurrence. Recurrence, n = 15; onset, n = 5. (**D**) Syt7 mRNA level in patients with different onset episodes. Mania, n = 7; depression, n = 11; hypomania, n = 1; non-specific, n = 1. (**E**) Syt7 mRNA level in patients with different types of episode when blood samples were collected. Mania, n = 7; depression, n = 6; mixed, n = 7. (**F**) Syt7 mRNA level in patients with or without suicidal tendencies. With, n = 10; without, n = 10. (**G**) Syt7 mRNA level in the blood cells of BD patients. Of the 20 patients that underwent plasma tests, 16 had blood cells in storage and thus were tested for Syt7 mRNA expression in their blood cells. HC, n = 11; BD-I, n = 16. Student's *t*-test. **P* < 0.05; error bars, s.e.m.

Table S1. Clinical characteristics of blood donors with bipolar disorder

Sample ID	Gender	Age	FH	SI	Onset	Feature of 1st E	Feature of this time	Psych-osis	Diag-nosis	Course of illness (month)	Hyper-insulinism	Hyper-lipidemia	Hyper-uricemia	High BMI
BD#01	F	17	N	N	1st E	Depression	Mixed	Y	BD II	6	Unk	N	Y	N
BD#02	F	26	N	Y	1st E	Depression	Mixed	N	BD II	60	N	N	N	Y
BD#03	F	16	Y	N	R	Depression	Mixed	N	BD II	60	Unk	Unk	Unk	N
BD#04	M	34	Y	N	R	Depression	Depression	Y	BD I	120	N	Y	N	Y
BD#05	F	20	Y	Y	R	Hypomania	Mixed	N	BD I	72	Y	Y	Y	Y
BD#06	M	31	Y	Y	R	Unspecified features	Depression	Y	BD I	24	Y	N	Y	Y
BD#07	M	30	N	Y	R	Mania	Depression	Y	BD I	60	N	N	N	N
BD#08	F	31	N	N	R	Mania	Mania	N	BD I	8	Y	N	N	Y
BD#09	M	17	N	N	R	Mania	Mania	Y	BD I	24	N	N	N	N
BD#10	F	21	Y	Y	R	Depression	Mixed	N	BD I	7	N	N	N	N
BD#11	F	20	N	Y	R	Depression	Mixed	N	BD I	8	N	N	N	N
BD#12	F	19	N	N	1st E	Mania	Mania	N	BD I	8	N	Y	N	N
BD#13	F	20	N	N	1st E	Mania	Mania	N	BD I	1	Unk	Unk	Unk	N
BD#14	M	14	N	N	R	Depression	Mania	Y	BD I	24	N	Y	Unk	N
BD#15	M	18	N	Y	R	Mania	Mania	N	BD I	1	N	N	N	N
BD#16	M	21	N	N	R	Mania	Depression	N	BD I	72	N	Y	N	Unk
BD#17	F	23	N	Y	1st E	Depression	Mixed	Y	BD I	6	N	N	N	Unk
BD#18	F	22	Unk	Y	R	Depression	Depression	N	BD II	12	Y	N	N	N
BD#19	F	16	Unk	Y	R	Depression	Depression	Y	BD II	60	N	N	N	N
BD#20	F	23	Unk	N	R	Depression	Mania	N	BD II	60	Y	Unk	N	Y
Control #1	F	28	N	N	-	-	-	-	-	-	-	-	-	-

Control #2	F	26	N	N	-	-	-	-	-	-	-	-	-	-
Control #3	F	23	N	N	-	-	-	-	-	-	-	-	-	-
Control #4	M	29	N	N	-	-	-	-	-	-	-	-	-	-
Control #5	M	29	N	N	-	-	-	-	-	-	-	-	-	-
Control #6	M	24	N	N	-	-	-	-	-	-	-	-	-	-
Control #7	M	23	N	N	-	-	-	-	-	-	-	-	-	-
Control #8	M	27	N	N	-	-	-	-	-	-	-	-	-	-
Control #9	F	22	N	N	-	-	-	-	-	-	-	-	-	-
Control #10	F	25	N	N	-	-	-	-	-	-	-	-	-	-
Control #11	M	38	N	N	-	-	-	-	-	-	-	-	-	-

Note: FH = Family history; SI = Suicide ideation; M = Male; F = Female; R= Recurrence; 1st E= First episode; BD I = Bipolar I Disorder; Y=Yes; N=No; Unk = Unknown, there was insufficient information to determine these phenotypes.

Table S2. Sequence of primers used for qRT-PCR analysis.

Gene	Sequence (5' to 3')
AKT1 (human)	Forward: 5’-ACTCGGAGAAGAACGTGGTG-3’
	Reverse: 5’-GCCGTAGTCATTGTCCTCCA-3’
AKT2 (human)	Forward: 5’-CGCGACATCAAGCTGGAAAA-3’
	Reverse: 5’-CCGGCCATAGTCATTGTCCT-3’
C1QL3 (human)	Forward: 5’-TCCATCCCGGGCATCTACTT-3’
	Reverse: 5’-CTTCATCTCCCGGCTCCAAA-3’
CHL1 (human)	Forward: 5’-GGATCCGCCCAGAGCTTAC-3’
	Reverse: 5’-AGACAGGATTATGGTTTGCAGTT-3’
CPLX1 (human)	Forward: 5’-GCCAGGGCATCCGAGACA-3’
	Reverse: 5’-ATGCTCTCGTCCTCCTCCTC-3’
HAP1 (human)	Forward: 5’-GTGCTCAGGCTGGAAAACTATG-3’
	Reverse: 5’-TTTCAGTCTCAGCCCCATACATC-3’
MUSK (human)	Forward: 5’-AGACAGCCCTCTCAGGGAAA-3’
	Reverse: 5’-CCTGGCAAAAACCTCAACTTCC-3’
NLGN2 (human)	Forward: 5’-CCCGAGCGTATCACCATCTT-3’
	Reverse: 5’-ACTTGAGCGGCTGGTAGTTG-3’
PAK1 (human)	Forward: 5’-AACCTCTGCCTCCAAACCC-3’
	Reverse: 5’-GCATTCCCGTAAACTCCCCT-3’
PPARGC1A (human)	Forward: 5’-GCTGGCGAATCCAGTTTGTG-3’
	Reverse: 5’-AGATCTGGGCAAAGAGGCTG-3’
PSTPIP1 (human)	Forward: 5’-TCGCAGTGCAGGAGATACAG-3’
	Reverse: 5’-AGGTAGGAACCAGGGACGAA-3’
PTEN (human)	Forward: 5’-TGTAAAGCTGGAAAGGGACGA-3’
	Reverse: 5’-GGAATAGTTACTCCCTTTTTGTCTC-3’
RGMA (human)	Forward: 5’-GGCTAGTGGTAACAGGCCGA-3’
	Reverse: 5’-TTGAGGATCTTGCACGGGG-3’
RTN4RL2 (human)	Forward: 5’-GCCTGCAGTACCTCTACCTC-3’
	Reverse: 5’-GGAAGAGGTGGCTCAGGTTG-3’
SHANK1 (human)	Forward: 5’-GAAGTCCTACCAGGCCCAAG-3’
	Reverse: 5’-GAGAGCGATTCGCCACTTCT-3’
TBK1 (human)	Forward: 5’-ACAGATTTTGGTGCAGCTAGAGA-3’
	Reverse: 5’-TGTTACCCCAATGCTCCAAAGA-3’
UNC13A (human)	Forward: 5’-TCTGCTTTGCGTTGGAGTCA-3’
	Reverse: 5’-CACCGTCAGTCCCAAATCCA-3’
SYT7 (human)	Forward: 5’-AAGCGGGTGGAGAAGAAGAA-3’
	Reverse: 5’-CGAAGGCGAAGGACTCATTG-3’

Table S3. Statistical data for all experiments.

Fig. 1			
Fig.1B	AKT1	HC	1.00 ± 0.06, n = 4 cell lines of 4 subjects
		BD-I	0.79 ± 0.07, n = 6 cell lines of 6 subjects
	AKT2	HC	1.00 ± 0.10, n = 4 cell lines of 4 subjects
		BD-I	0.74 ± 0.11, n = 6 cell lines of 6 subjects
	C1QL3	HC	1.00 ± 0.34, n = 4 cell lines of 4 subjects
		BD-I	1.64 ± 1.41, n = 6 cell lines of 6 subjects
	CHL1	HC	1.00 ± 0.58, n = 4 cell lines of 4 subjects
		BD-I	4.10 ± 1.23, n = 6 cell lines of 6 subjects
	CPLX1	HC	1.00 ± 0.05, n = 4 cell lines of 4 subjects
		BD-I	1.48 ± 0.54, n = 6 cell lines of 6 subjects
	HAP1	HC	1.00 ± 0.30, n = 4 cell lines of 4 subjects
		BD-I	0.83 ± 0.35, n = 6 cell lines of 6 subjects
	MUSK	HC	1.00 ± 0.77, n = 4 cell lines of 4 subjects
		BD-I	0.43 ± 0.20, n = 6 cell lines of 6 subjects
	NLGN2	HC	1.00 ± 0.13, n = 4 cell lines of 4 subjects
		BD-I	0.93 ± 0.13, n = 6 cell lines of 6 subjects
	PAK1	HC	1.00 ± 0.29, n = 4 cell lines of 4 subjects
		BD-I	1.09 ± 0.34, n = 6 cell lines of 6 subjects
	PPARGC1A	HC	1.00 ± 0.27, n = 4 cell lines of 4 subjects
		BD-I	1.06 ± 0.29, n = 6 cell lines of 6 subjects
	PTEN	HC	1.00 ± 0.05, n = 4 cell lines of 4 subjects
		BD-I	1.00 ± 0.09, n = 6 cell lines of 6 subjects
	RGMA	HC	1.00 ± 0.09, n = 4 cell lines of 4 subjects
		BD-I	1.24 ± 0.38, n = 6 cell lines of 6 subjects
	RTN4RL2	HC	1.00 ± 0.12, n = 4 cell lines of 4 subjects
		BD-I	1.28 ± 0.43, n = 6 cell lines of 6 subjects
	SHANK1	HC	1.00 ± 0.16, n = 4 cell lines of 4 subjects
		BD-I	1.47 ± 0.47, n = 6 cell lines of 6 subjects
	SYT7	HC	1.00 ± 0.42, n = 4 cell lines of 4 subjects
		BD-I	0.64 ± 0.14, n = 6 cell lines of 6 subjects
	TBK1	HC	1.00 ± 0.05, n = 4 cell lines of 4 subjects
		BD-I	0.96 ± 0.04, n = 6 cell lines of 6 subjects
	UNC13A	HC	1.00 ± 0.07, n = 4 cell lines of 4 subjects
		BD-I	0.60 ± 0.13 n = 6 cell lines of 6 subjects
Fig.1C	AKT1	HC	1.00 ± 0.10, n = 4 cell lines of 4 subjects
		BD-I	0.80 ± 0.21, n = 6 cell lines of 6 subjects
	AKT2	HC	1.00 ± 0.18, n = 4 cell lines of 4 subjects

		BD-I	0.96 ± 0.29, n = 6 cell lines of 6 subjects
	C1QL3	HC	1.00 ± 0.89, n = 4 cell lines of 4 subjects
		BD-I	0.04 ± 0.02, n = 6 cell lines of 6 subjects
	CHL1	HC	1.00 ± 0.57, n = 4 cell lines of 4 subjects
		BD-I	6.23 ± 4.16, n = 6 cell lines of 6 subjects
	CPLX1	HC	1.00 ± 0.49, n = 4 cell lines of 4 subjects
		BD-I	0.88 ± 0.41, n = 6 cell lines of 6 subjects
	HAP1	HC	1.00 ± 0.58, n = 4 cell lines of 4 subjects
		BD-I	0.05 ± 0.05, n = 6 cell lines of 6 subjects
	MUSK	HC	1.00 ± 0.60, n = 4 cell lines of 4 subjects
		BD-I	0.55 ± 0.15, n = 6 cell lines of 6 subjects
	NLGN2	HC	1.00 ± 0.27, n = 4 cell lines of 4 subjects
		BD-I	1.16 ± 0.35, n = 6 cell lines of 6 subjects
	PAK1	HC	1.00 ± 0.13, n = 4 cell lines of 4 subjects
		BD-I	0.26 ± 0.07, n = 6 cell lines of 6 subjects
	PPARGC1A	HC	1.00 ± 0.30, n = 4 cell lines of 4 subjects
		BD-I	1.68 ± 0.51, n = 6 cell lines of 6 subjects
	PSTPIP1	HC	1.00 ± 0.30, n = 4 cell lines of 4 subjects
		BD-I	1.39 ± 0.68, n = 6 cell lines of 6 subjects
	PTEN	HC	1.00 ± 0.05, n = 4 cell lines of 4 subjects
		BD-I	1.17 ± 0.16, n = 6 cell lines of 6 subjects
	RGMA	HC	1.00 ± 0.11, n = 4 cell lines of 4 subjects
		BD-I	4.36 ± 1.69, n = 6 cell lines of 6 subjects
	RTN4RL2	HC	1.00 ± 0.43, n = 4 cell lines of 4 subjects
		BD-I	0.62 ± 0.22, n = 6 cell lines of 6 subjects
	SHANK1	HC	1.00 ± 0.55, n = 4 cell lines of 4 subjects
		BD-I	0.59 ± 0.27, n = 6 cell lines of 6 subjects
	SYT7	HC	1.00 ± 0.02, n = 4 cell lines of 4 subjects
		BD-I	0.42 ± 0.08, n = 6 cell lines of 6 subjects
	TBK1	HC	1.00 ± 0.06, n = 4 cell lines of 4 subjects
		BD-I	0.98 ± 0.21, n = 6 cell lines of 6 subjects
	UNC13A	HC	1.00 ± 0.47, n = 4 cell lines of 4 subjects
		BD-I	0.69 ± 0.44, n = 6 cell lines of 6 subjects
Fig.1D	WT	176.4 ± 13.8 s, n = 10	
	C1QL3	172.0 ± 14.1 s, n = 10	
	HAP1	168.6 ± 8.3 s, n = 10	
	MUSK	175.7 ± 12.6 s, n = 10	
	PAK1	173.8 ± 9.1 s, n = 10	
	PPARGC1A	174.8 ± 8.4 s, n = 10	
	RTN4RL2	178.6 ± 14.0 s, n = 10	

	SHANK1	174.4 ± 11.0 s, n = 10
	SYT7	139.8 ± 10.3 s, n = 10; p<0.05, compared to WT
	UNC13A	170.0 ± 10.8 s, n = 10
	CHL1	172.6 ± 10.4 s, n = 10
	RGMA	167.5 ± 7.3 s, n = 10
Fig. 2		
Fig.2A	HC	1.00 ± 0.03, n = 4 cell lines of 4 subjects
	LR	0.44 ± 0.01, n = 3 cells lines of 3 patients; p<0.05, compared to HC
	NR	0.39 ± 0.03, n = 3 cell lines of 3 subjects; p<0.001, compared to HC
Fig.2B	HC	0.45 ± 0.03, n = 4 cell lines of 4 subjects
	LR	0.15 ± 0.06, n = 3 cells lines of 3 patients; p<0.02, compared to HC
	NR	0.08 ± 0.03, n = 3 cell lines of 3 subjects; p<0.001, compared to HC
Fig.2C	HC	1.00 ± 0.16, n = 3 cell lines of 3 subjects
	LR	0.49 ± 0.01, n = 3 cell lines of 3 subjects
	NR	0.23 ± 0.02, n = 3 cell lines of 3 subjects; p<0.04, compared to HC
Fig.2D (Left)	Dark	WT: 138.9 ± 9.1 s, n = 12
		Syt7 KO: 58.9 ± 8.0 s, n = 17, p<0.001
	Light	WT: 154.5 ± 7.7 s, n = 12
		Syt7 KO: 221.1 ± 10.2 s, n = 17, p<0.001
Fig.2D (Mid)	Dark	WT: 138.9 ± 9.1 s, n = 12
		Syt7 KO: 52.5 ± 9.4 s, n = 8, p<0.001
	Light	WT: 154.5 ± 7.7 s, n = 12
		Syt7 KO: 74.1 ± 10.1 s, n = 8, p<0.001
Fig.2E	Dark	WT: 223.2 ± 8.6 s, n = 12
		Syt7 KO: 165.5 ± 11.1 s, n = 12, p<0.01
	Light	WT: 190.9 ± 21.4 s, n = 12
		Syt7 KO: 247.6 ± 8.4 s, n = 12, p<0.05
Fig.2F	Dark	WT: 30.9 ± 4.8%, n = 8
		Syt7 KO: 13.8 ± 3.2%, n = 9, p<0.02
	Light	WT: 38.1 ± 6.1%, n = 8
		Syt7 KO: 55.6 ± 4.8%, n = 9, p<0.05
Fig.2G	Dark	WT: 79.6 ± 3.1%, n = 8
		Syt7 KO: 88.7 ± 2.8%, n = 8, p<0.04
	Light	WT: 80.8 ± 3.3%, n = 8
		Syt7 KO: 64.1 ± 5.9%, n = 8, p<0.03
Fig.2H	Dark	WT: 227.3 ± 18.9 s, n = 10
		Syt7 KO: 314.2 ± 22.1 s, n = 10, p<0.02
	Light	WT: 272.1 ± 31.3 s, n = 12

			Syt7 KO: 172.5 ± 33.9 s, n = 12, p<0.01
Fig.2I (Left)	Dark		WT: 97.1 ± 19.3, n = 8
			Syt7 KO: 64.2 ± 7.5, n = 8, p>0.14
	Light		WT: 76.6 ± 10.5, n = 8
			Syt7 KO: 57.4 ± 8.2, n = 8, p>0.17
Fig.2I (Right)	Night	71dB	WT: 0.48 ± 0.05, n = 8
			Syt7 KO: 0.31 ± 0.06, n = 8, p<0.04
		74dB	WT: 0.59 ± 0.04, n = 8
			Syt7 KO: 0.48 ± 0.06, n = 8, p>0.1
		80dB	WT: 0.73 ± 0.05, n = 8
			Syt7 KO: 0.57 ± 0.06, n = 8, p<0.04
	Day	71dB	WT: 0.53 ± 0.07, n = 8
			Syt7 KO: 0.33 ± 0.07, n = 8, p<0.04
		74dB	WT: 0.65 ± 0.05, n = 8
			Syt7 KO: 0.50 ± 0.05, n = 8, p<0.05
		80dB	WT: 0.75 ± 0.02, n = 8
			Syt7 KO: 0.53 ± 0.08, n = 8, p<0.01
Fig.3			
Fig.3A	Night	WT	Saline: 126.5 ± 5.5 s, n = 8
			0.2 mg/kg B.W.: 199.88 ± 12.88 s, n = 8; p<0.001, compared to WT saline
			0.5 mg/kg B.W.: 209.50 ± 8.29 s, n = 8; p<0.001, compared to WT saline
			1.0 mg/kg B.W.: 223.38 ± 11.37 s, n = 8; p<0.001, compared to WT saline
		KO	Saline: 71.63 ± 5.71 s, n = 8; p<0.001, compared to WT
			0.2 mg/kg B.W.: 114.38 ± 12.35 s, n = 8; p<0.001, compared to KO saline, compared to WT 0.2 mg/kg
			0.5 mg/kg B.W.: 211.75 ± 6.08 s, n = 8; p<0.001, compared to KO saline; p>0.1, compared to WT 0.5 mg/kg
			1.0 mg/kg B.W.: 227.00 ± 14.62 s, n = 8; p<0.001, compared to KO saline; p>0.1, compared to WT 1.0 mg/kg
Fig.3B	Day	WT	Saline: 128.00 ± 11.39 s, n = 8
			0.2 mg/kg B.W.: 187.75 ± 10.88 s, n = 8; p>0.05, compared to WT saline
			0.5 mg/kg B.W.: 241.88 ± 11.13 s, n = 8; p<0.001, compared to WT saline
			1.0 mg/kg B.W.: 271.75 ± 8.58 s, n = 8; p<0.001, compared to WT saline
		KO	Saline: 222.38 ± 11.80 s, n = 8; p<0.001, compared to WT saline
			0.2 mg/kg B.W.: 184.75 ± 9.38 s, n = 8; p<0.001, compared to KO saline; p>0.83, compared to WT 0.2 mg/kg
			0.5 mg/kg B.W.: 243.88 ± 8.71 s, n = 8; p<0.001, compared to KO

			saline; p>0.88, compared to WT 0.5 mg/kg
			1.0 mg/kg B.W.: 267.38 ± 9.25 s, n = 8; p<0.001, compared to KO saline; p>0.73, compared to WT 1.0 mg/kg
Fig.3C	Dark	WT	Saline: 30.9 ± 4.8%, n = 8
			OLZ: 82.8 ± 8.8%, n = 8; p<0.01
		KO	Saline: 13.8 ± 3.2%, n = 9
			OLZ: 70.3 ± 11.0%, n = 9; p<0.01
	Light	WT	Saline: 38.1 ± 6.1%, n = 8
			OLZ: 61.3 ± 7.7%, n = 8; p<0.04
		KO	Saline: 55.6 ± 4.8%, n = 9
			OLZ: 73.9 ± 5.3%, n = 9; p<0.03
Fig.3D	Dark	WT	Saline: 80.7 ± 1.8%, n = 10
			OLZ: 68.7 ± 5.3%, n = 10; p<0.05
		KO	Saline: 88.9 ± 1.9%, n = 10
			OLZ: 73.8 ± 6.6%, n = 10; p<0.05
	Light	WT	Saline: 80.4 ± 2.0%, n = 10
			OLZ: 65.4 ± 4.6%, n = 10; p<0.02
		KO	Saline: 71.2 ± 3.6%, n = 10
			OLZ: 60.6 ± 3.5%, n = 10; p<0.05
Fig.3E	Dark	WT	Saline: 248.1 ± 15.0 s, n = 11
			OLZ: 195.8 ± 17.2 s, n = 11; p<0.04
		KO	Saline: 290.7 ± 14.8 s, n = 11
			OLZ: 176.3 ± 37.2 s, n = 11; p<0.02
	Light	WT	Saline: 292.6 ± 12.9 s, n = 11
			OLZ: 191.6 ± 24.8 s, n = 11; p<0.01
		KO	Saline: 236.5 ± 29.7 s, n = 11
			OLZ: 127.4 ± 29.0 s, n = 11; p<0.02
Fig.3F	Dark	WT	Saline: 122.8 ± 9.7, n = 8
			Li_2CO_3: 125.2 ± 5.7, n = 8; p>0.1
		KO	Saline: 65.2 ± 9.6, n = 8
			Li_2CO_3: 55.5 ± 12.5, n = 9; p>0.1
	Light	WT	Saline: 139.0 ± 10.8, n = 8
			Li_2CO_3: 128.3 ± 3.8, n = 8; p>0.1
		KO	Saline: 148.0 ± 4.8, n = 8
			Li_2CO_3: 174.7 ± 13.9, n = 8; p>0.1
Fig.3G	Dark	WT	Saline: 30.0 ± 8.9%, n = 8
			Li_2CO_3: 70.9 ± 12.7%, n = 8; p<0.03
		KO	Saline: 15.0 ± 6.7%, n = 8
			Li_2CO_3: 44.4 ± 11.0%, n = 8; p<0.05
	Light	WT	Saline: 42.5 ± 9.9%, n = 8

			Li_2CO_3: 89.4 ± 5.8%, n = 8; p<0.01
		KO	Saline: 56.6 ± 12.2%, n = 8
			Li_2CO_3: 81.6 ± 6.2%, n = 8; p<0.05
Fig.3H	Dark	WT	Saline: 80.9 ± 3.4%, n = 8
			Li_2CO_3: 63.9 ± 3.8%, n = 8; p<0.01
		KO	Saline: 91.7 ± 2.2%, n = 8
			Li_2CO_3: 72.5 ± 3.6%, n = 8; p<0.001
	Light	WT	Saline: 80.9 ± 3.5%, n = 8
			Li_2CO_3: 61.8 ± 6.3%, n = 8; p<0.03
		KO	Saline: 74.8 ± 2.6%, n = 8
			Li_2CO_3: 60.4 ± 5.1%, n = 8; p<0.04
Fig.3I	Dark	WT	Saline: 267.9 ± 12.7, n = 8
			Li_2CO_3: 218.2 ± 21.8, n = 8; p>0.5
		KO	Saline: 237.1 ± 17.0, n = 8
			Li_2CO_3: 135.5 ± 23.8, n = 8; p<0.01
	Light	WT	Saline: 233.3 ± 4.6, n = 8
			Li_2CO_3: 261.5 ± 22.6; n = 8; p>0.5
		KO	Saline: 270.0 ± 14.8, n = 8
			Li_2CO_3: 188.8 ± 11.4, n = 8; p<0.01
Fig. 4			
Fig.4B (Right)	HC		9.77 ± 1.37, n = 11 subjects
	BD		5.83 ± 0.71, n = 20 subjects; p<0.001
Fig.4C (Right)	HC		1.00 ± 0.14, n = 11
	BD-I		0.69 ± 0.08, n = 14; p<0.05
	BD-II		0.37 ± 0.13, n = 6; p<0.01
Fig.4D (Right)	HC		1.00 ± 0.14, n = 11
	With psychosis		0.56 ± 0.09, n = 12; p<0.02
	w/o psychosis		0.65 ± 0.12, n = 8; p>0.09
Fig.4E (Right)	HC		1.00 ± 0.14, n = 11
	With family history		0.61 ± 0.09, n = 12; p<0.03
	w/o history		0.77 ± 0.09, n = 5; p>0.3
Fig.4F (Right)	HC		1.00 ± 0.14, n = 11
	Untreated		0.44 ± 0.21, n = 4; p<0.05
	Treated		0.64 ± 0.07, n = 16; p<0.02
Supplementary Fig.1			
Fig.S1A	WT		3999.03±290.97 cm, n=10
	C1QL3		3922.53±144.57 cm, n=10
	HAP1		3981.35±144.70 cm, n=10

	MUSK		4052.11±213.84 cm, n=10
	PAK1		4193.98±353.39 cm, n=10
	PPARGC1A		3510.23±282.45 cm, n=10
	RTN4RL2		3816.16±429.38 cm, n=10
	SHANK1		4127.11±340.85 cm, n=10
	SYT7		5400.37±324.76 cm, n=10; p<0.005, compared to WT
	UNC13A		4136.44±358.02 cm, n=10
	CHL1		4099.43±379.56 cm, n=10
	RGMA		4087.69±326.69 cm, n=10
Fig.S1B	WT		44.70±3.90 s, n=10
	C1QL3		37.17±3.56 s, n=10
	HAP1		32.04±3.44 s, n=10
	MUSK		45.44±4.22 s, n=10
	PAK1		70.44±10.22 s, n=10; p<0.05, compared to WT
	PPARGC1A		62.28±11.34 s, n=10
	RTN4RL2		43.70±7.91 s, n=10
	SHANK1		52.88±7.64 s, n=10
	SYT7		86.63±12.78 s, n=10; p<0.005, compared to WT
	UNC13A		49.23±4.87 s, n=10
	CHL1		59.21±16.44 s, n=10
	RGMA		36.46±5.07 s, n=10
Fig.S1D	Dark		WT: 5140.2 ± 570.2, n = 8
			Syt7 KO: 6999.5 ± 804.0, n = 8, p<0.05
	Light		WT: 918.6 ± 127.9, n = 8
			Syt7 KO: 584.6 ± 90.3, n = 8, p<0.05
Supplementary Fig.2			
Fig.S2A	WT		24.5 ± 0.6 g, n = 17
	Syt7 KO		21.2 ± 0.6 g, n = 14, p<0.001
Fig.S2B	WT		0.187 ± 0.003 g/day/g body weight, n = 12
	Syt7 KO		0.212 ± 0.007 g/day/g body weight, n = 12, p<0.01
Fig.S2C	Dark	WT	4.02 ± 0.13 $X10^3$ ml/h/g, n = 8
		Syt7 KO	4.55 ± 0.14 $X10^3$ ml/h/g, n = 8, p<0.02
	Light	WT	3.58 ± 0.15 $X10^3$ ml/h/g, n = 8
		Syt7 KO	3.10 ± 0.12 $X10^3$ ml/h/g, n = 8, p<0.03
Fig.S2D	Dark	WT	3.58 ± 0.07 $X10^3$ ml/h/g, n = 8
		Syt7 KO	3.86 ± 0.11 $X10^3$ ml/h/g, n = 8, p<0.05
	Light	WT	2.75 ± 0.17 $X10^3$ ml/h/g, n = 8
		Syt7 KO	2.54 ± 0.09 $X10^3$ ml/h/g, n = 8, p>0.2
Supplementary Fig.3			
Fig.S3A	HC-F		1.00 ± 0.16, n = 4
	BD-F		0.53 ± 0.08, n = 13; p<0.02

	HC-M	1.00 ± 0.21, n = 7
	BD-M	0.69 ± 0.13, n = 7; p>0.25
Fig.S3B	HC<30	1.00 ± 0.20, n = 7
	BD<30	0.56 ± 0.08, n = 16; p<0.02
	HC>30	1.00 ± 0.21, n = 4
	BD>30	0.79 ± 0.07, n = 4; p>0.37
Fig.S3C	HC	1.00 ± 0.14, n = 11
	Recurrence	0.63 ± 0.09, n = 15; p<0.03
	Onset	0.51 ± 0.14, n = 5; p<0.05
Fig.S3D	HC	1.00 ± 0.14, n = 11
	Depression	0.62 ± 0.11, n = 11; p<0.05
	Mania	0.56 ± 0.12, n = 7; p<0.05
Fig.S3E	HC	1.00 ± 0.14, n = 11
	Mixed	0.65 ± 0.12, n = 7; p>0.1
	Depression	0.58 ± 0.14, n = 6; p>0.06
	Mania	0.55 ± 0.14, n = 7; p<0.05
Fig.S3F	HC	1.00 ± 0.14, n = 11
	w/o suicidal tendency	0.51 ± 0.12, n = 10; p<0.02
	with suicidal tendency	0.68 ± 0.08, n = 10; p>0.07
Fig.S3G	HC	0.53 ± 0.12, n = 11
	BD-I	0.12 ± 0.04, n = 16; p<0.02